Liver International

WILEY

Liver INTERNATIONAL

ORIGINAL ARTICLE OPEN ACCESS

CD44 in Group 1 Innate Lymphoid Cells Impacts the Development and Progression of Steatohepatitis

Manon Bourinet[1] | Elodie Vieira[1] | Déborah Rousseau[1] | Stéphanie Bonnafous[2] | Fréderic Soysouvanh[1] | Axelle Strazzulla[1] | Coline Elliot[1] | Stéphanie Patouraux[2] | Pierre S. Leclère[1] | Iryna Moskalevska[3] | Julien Cherfils-Vicini[3] | Meri K. Tulic[1] | Matthias Mack[4] | Béatrice Bailly-Maitre[1] | Véronique Orian-Rousseau[5] | Antonio Iannelli[2] | Arnauld Belmer[1] | Albert Tran[2] | Rodolphe Anty[2] | Philippe Gual[1] | Carmelo Luci[1]

[1]Université Côte d'Azur, INSERM U1065, C3M, Nice, France | [2]Université Côte d'Azur, CHU, INSERM U1065, C3M, Nice, France | [3]Université Côte d'Azur, IRCAN, CNRS 7284, Inserm U1081, IHU RESPIRera, Nice, France | [4]Department of Internal Medicine II, Division of Nephrology, University Hospital Regensburg, Regensburg, Germany | [5]Karlsruhe Institute of Technology (KIT), Institute of Biological and Chemical Systems–Functional Molecular Systems (IBCS-FMS), Karlsruhe, Germany

Correspondence: Philippe Gual (philippe.gual@inserm.fr) | Carmelo Luci (carmelo.luci@inserm.fr)

Received: 11 March 2025 | **Revised:** 19 June 2025 | **Accepted:** 14 August 2025

Handling Editor: Luca Valenti

Funding: This work was supported by grants from Institut National de la santé et de la Recherche Médicale (INSERM), Université Côte d'Azur and various charities (Association Française pour l'Etude du Foie (AFEF) to PG and CL). This work was also funded by the French Government (National Research Agency, ANR): #ANR-18-CE14-0019-02, #ANR-19-CE14-0044-01, #ANR-21-CE14-0015-03, #ANR-22-CE14-0027-01, #ANR-23-CE14-0048-03 and through the "Investments for the Future" LABEX SIGNALIFE (#ANR-11-LABX-0028-01) and the UCA^{JEDI} Investments in the Future project (#ANR-15-IDEX-0001) and German Government (Deutsche Forschungsgemeinschaft DFG OR124/21-1). EV was supported by a PhD grant from the Fondation pour la Recherche Médicale (FRM) and MB by the ANR (#ANR-18-CE14-0019-02). MB is currently supported by a doctoral fellowship from the French Ministry of Research and from the Fondation pour la Recherche Médicale (FRM).

Keywords: ILC1s | inflammation | MASH | MASLD | NAFLD | NK cells | steatohepatitis

ABSTRACT

Background and Aims: Innate lymphoid cells (ILCs) play pivotal roles in inflammation and fibrosis, which are key features of chronic liver diseases. The contribution of group 1 ILCs, including natural killer (NK) cells and helper-like ILC1s, to liver inflammation during steatohepatitis and metabolic dysfunction-associated steatotic liver diseases (MASLD) is still a matter of debate and requires further investigation.

Methods: We engineered a mouse model of specific deficiency of CD44 in group 1 ILCs and challenged mice with diet-induced obesity and MASLD or diet-induced steatohepatitis. We performed in vitro studies and co-cultured LPS-stimulated liver NK cells with hepatocytes and macrophages to analyse the inflammatory response.

Abbreviations: ALT, Alanine aminotransferase; AST, Aspartate aminotransferase; BMI, Body Mass Index; CCL2, Chemokine CC ligand 2; CCL5, Chemokine CC ligand 5; CD, Control diet; Clec2, C-type lectin domain family 2; Col1a1, Collagen type 1 alpha 1; Csf2, Colony-stimulated factor 2; CXCL1, CXC motif chemokine ligand 1; CXCL10, CXC motif chemokine ligand 10; FMO, Fluorescence Minus One; GM-CSF, Granulocyte Macrophages Colony Stimulating Factor; H&E, Haematoxylin and Eosin; HCV, Hepatitis C virus; HFD, High-fat diet; HOMA-IR, Homeostatic model assessment index; IFNγ, gamma Interferon; IL-6, Interleukin-6; ILCs, Innate Lymphoid Cells; KC, Kupffer Cells; KO, Knock-Out; LPS, Lipopolysaccharide; LSEC, Liver Sinusoidal Endothelial Cells; LTi, Lymphoid Tissue-Inducer cells; MASH, Metabolic dysfunction-associated steatohepatitis; MASLD, Metabolic dysfunction-associated steatotic liver disease; MCDD, Methionine and Choline-deficient diet; NAS, NAFLDactivity score; Ncr1, Natural cytotoxicity triggering receptor 1; NK, Natural Killer; Nkp46, Natural killer cell p46-related protein; Nos2, Nitric oxide synthase 2; OPN, Osteopontin; PRRs, Pattern Recognition Receptors; Spp1, secreted phosphoprotein 1; STAT, signal transducer and activator of transcription; Tgfb, Transforming growth factor beta; Timp1, TIMP Metallopeptidase inhibitor 1; TIM4, T-cell membrane protein 4; TLR, Toll like receptor; TNFα, Tumour Necrosis Factor alpha; TRAIL, Tumour-Necrosis-factor related apoptosis inducing ligand; WT, Wild Type.

Philippe Gual and Carmelo Luci authors jointly supervised this work.

Results: As group 1 ILCs expressed the cell surface molecule CD44, its specific targeting was used to investigate if CD44 could affect the development of liver inflammation. Here, we found that CD44 deficiency in group 1 ILCs was sufficient to decrease the absolute number of hepatic NKp46$^+$ ILCs, NK cells and ILC1s in chow diet and in response to diet induced-MASLD or steatohepatitis. CD44 deficiency in group 1 ILCs aggravated liver complications by exacerbating hepatic injury, inflammation, and fibrosis, which was also associated with inflammatory and osteopontin$^+$ macrophages accumulation. The absence of CD44 in NK cells enhanced their inflammatory phenotypes in response to LPS, which in turn triggered release of pro-inflammatory mediators by hepatocytes and macrophages.

Conclusions: Our findings reveal a novel role for CD44 in regulating the dynamics of group 1 ILCs, which in turn affects steatohepatitis and MASLD development.

1 | Introduction

Metabolic dysfunction-associated steatotic liver disease (MASLD) is the leading cause of chronic liver disease, with an alarming worldwide increase in prevalence [1]. These liver abnormalities range from hepatic steatosis, defined by lipid accumulation in hepatocytes, to metabolic dysfunction-associated steatohepatitis (MASH). The chronic inflammatory status and elevated liver injury associated with MASH are key players in its progression to more severe liver abnormalities such as fibrosis/cirrhosis and hepatocellular carcinoma [2, 3]. Extra-hepatic inflammation (e.g., gut and adipose tissue) is involved in the changes in liver immune cell composition and activity related to the chronic inflammation that leads to MASLD progression. Numerous immune cells and reactions have been identified as drivers of this inflammation, although the role of ILCs and their regulation remain poorly understood [2, 3].

Innate lymphoid cells (ILCs) are part of innate immunity and are well equipped to quickly respond to local injury and shape immune responses, as well as maintain epithelial integrity and tissue repair [4]. ILC subsets are defined as the innate counterparts of T lymphocytes and consist of a family of cells divided into 5 subsets, namely, Natural Killer (NK) cells, ILC1s, ILC2s, ILC3s and lymphoid tissue-inducer cells (LTi) [5–8]. Most of them are cytokine producers and tissue-resident cells except for circulating cytotoxic NK cells [9]. Accumulating evidence indicated that cellular metabolism (glycolysis, oxidative respiration, fatty acid oxidation) is required for the activation of NK cells [10]. During the course of an immune response, NK cells undergo metabolic reprogramming that supports their functions, and this is greatly influenced by the environment, as recently demonstrated during diseases such as cancer, infection or obesity [3, 11, 12]. NK cells and ILC1s share expression of several markers, such as the activating receptor NKp46 [13]. These cells play important roles in host protection against pathogens and tumours and were recently implicated in metabolic disorders [3]. In the liver, the contribution of NKp46$^+$ cells to the onset and progression of hepatic abnormalities in diet-induced MASLD is a matter of debate, presumably due to their phenotypical and functional heterogeneity [13–15]. To propose new therapeutic targets against steatohepatitis, we previously identified cluster of differentiation 44 (CD44) as a key player in regulating hepatic inflammation during chronic liver diseases. CD44 is a cell-surface glycoprotein involved in cell–cell interactions, cell adhesion, migration, activation and is mainly expressed on immune cells such as T cells, macrophages and neutrophils [16–18]. It also contributes to leukocyte recruitment to inflammatory sites, and its targeting can limit the inflammatory response [19]. The role of CD44 in the physiology of T lymphocytes and macrophages is becoming better understood [20–23]. In this way, we recently showed that, using a mouse model of diet-induced MASH and alcohol-related liver disease (ALD), targeting CD44 (deficiency or antibody neutralisation) partially corrects MASH and improves liver inflammation in ALD by reducing macrophage activation and neutrophil mobilisation and functions, respectively [17, 18]. However, the relative contribution of other CD44$^+$ liver cells, including ILCs, to the development and progression of MASLD remains elusive, as does its contribution to ILC behaviour. Determining whether targeting CD44 on ILCs is beneficial or detrimental in pathological conditions could improve our understanding of the physiopathology of chronic liver diseases.

Here we investigated the dynamics of liver NKp46$^+$ ILCs in mouse models of MASH and steatohepatitis. Given that CD44 is crucial for the regulation of hepatic inflammation, we hypothesised that CD44 could influence NKp46$^+$ ILC behaviour and in turn, MASLD development. To address this issue, we generated a mouse model of NKp46-specific *Cd44* deletion (*Ncr1*$^{iCre/+}$ *Cd44*$^{flox/flox}$) and found that hepatic NKp46$^+$ ILC numbers are affected compared to littermate mice, with an increased number of pro-inflammatory liver macrophages and aggravated liver injury and fibrosis upon diet-induced MASH challenge. Further, LPS treatment of NK cells enhances their metabolic and inflammatory status when CD44 is deleted, which in turn makes hepatocytes and macrophages more prone to produce inflammatory cytokines. Our data indicated that CD44 on NKp46$^+$ ILCs may regulate their functions and responses involved in the crosstalk between liver cells during MASLD development.

2 | Methods

2.1 | Animals and Study Design

C57BL/6J/Rj wild-type, *Ncr1*$^{iCre/+}$ *CD44*$^{flox/flox}$ and littermate control Ncr*1*$^{+/+}$ *Cd44*$^{flox/flox}$ mice were acclimated under a 12/12 h light/dark cycle at a temperature of 21° ± 2°C. We used male mice as they show more stable hormone levels than females, particularly regarding sex hormones. In addition, male laboratory mice are generally more susceptible to develop diet-induced obesity and MASH [24–26]. *Ncr1*$^{iCre/+}$*Cd44*$^{flox/flox}$ mice were obtained at Mendelian frequencies, developed normally

Summary

- Liver inflammation is a key event in the development and progression of metabolic dysfunction-associated steatotic liver diseases (MASLD).
- Our work highlights a change in the liver frequency of Natural Killer Cells (NK cells) and Type 1 innate lymphoid cells (ILC1s) during the development of metabolic steatohepatitis (MASH).
- The cellular protein CD44 regulates their mobilisation and functions, with its specific deletion in NK cells and ILC1s aggravating liver abnormalities.
- Our research helps to understand the tight regulation of inflammation during chronic liver diseases.

and were fertile. Littermate mice and *CD44*$^{flox/flox}$*Ncr1*$^{Cre/+}$ male mice were fed *ad libitum* either a Western Diet (diet from Ssniff #S8926-E060 EF Western diet, +0.5% Cholesterol, custom-made) or chow diet (CD), with drinking water supplemented with 15% fructose for 10 or 24 weeks. Mice were also fed *ad libitum* either a methionine and choline-deficient diet (MCDD) or control diet (CD) for 2, 4, or 7 weeks (diets from Ssniff: #E15653-94 EF MCD | without Methionine/Choline, #E15654-04 EF CONTROL Methionine/Choline). *Ncr1*^{iCre} mice were provided by Pr. E. Vivier (CIML, Marseille, France) and *Cd44*$^{flox/flox}$ mice were previously described [27, 28]. The sequence encoding 'codon-improve' iCre recombinase is inserted into the 3′ untranslated region of *Ncr1* (which encodes NKp46). *Ncr1*^{iCre} mice were bred with *Cd44*$^{flox/flox}$ to generate NKp46$^{iCre/+}$ CD44$^{flox/flox}$, NKp46$^{+/+}$CD44$^{flox/flox}$ and NKp46$^{iCre/+}$ littermates. C57BL/6JRj wild-type were purchased from Janvier Labs (Le Genest-Saint-Isle, France). All mice were bred in our pathogen-free animal facility. The local ethics committee (CIEPAL n°28, Nice Côte d'Azur, France) approved the animal experiments.

2.2 | Transaminases Analysis

Serum ALT levels were determined using standardised UV tests after activation and serum triglyceride levels were determined by enzymatic colorimetric assay (Roche-Hitachi analyser Cobas 8000, Meylan, France).

2.3 | Mouse Tissue Sampling and Preparation

When sampled, one part of the mouse liver was immediately frozen in liquid nitrogen and stored at −80°C until analysis. Another part was fixed in buffered formalin, paraffin-embedded, sectioned, and stained with Haematoxylin–Eosin. A third part was cut, homogenised, and crushed on a cell-stainer (100 μm) and washed with RPMI 1640 medium. The cellular suspension was resuspended and centrifuged on a density cushion of Percoll (40% and 70%) at 780 g for 20 min at RT. FNP rings at the Percoll interface were collected and red blood cells were lysed with red blood cell lysis buffer (Sigma-Aldrich) for 5 min at RT. Cells were centrifuged and cell pellets resuspended in PBS EDTA (5 mM), FBS (3%). The success of the isolation was analysed by cell viability test (Trypan Blue exclusion test).

2.4 | Flow Cytometry

Cell suspensions were incubated with purified anti-FcγRII/III mAb blocking antibody before being stained at 4°C for 10 min to block Fc receptors. Then, cells were stained with fluorochrome-coupled antibodies for 30 min at 4°C. The following conjugated antibodies were purchased from BD Biosciences, Biolegend and Thermo Scientific: CD3 (PerCy5.5, clone 145-2C11, 551 163, BD Biosciences), CD19 (PerCy5.5, clone 1D3, 551 001, BD Biosciences), CD11b (PE-Cy7, clone M1/70, 552 850, BD Biosciences), CD11c (APC, clone N418, 17–0114-81, Thermo Scientific), CD44 (BV605, clone IM7, 563 151, BD Biosciences), CD45 (APCe780, clone 30-F11, 47–0451-82, Thermo Scientific), CD49a (A647, clone Ha31/8, 562 113, BD Biosciences), CD49b (FITC, clone DX5, 553 857, BD Biosciences), CD335/NKp46 (e450, clone 29A1.4, 48–3351-82, Thermo Scientific), F4/80 (FITC, clone BM8, 11–4801-85, Thermo Scientific), Ly6G (PerCy5.5, clone 1A8, 560 602, BD Biosciences), Ly6C (BV421, clone AL-21, 562 727, BD Biosciences), CLEC2A (PE, clone 17D9, 146 104, Biolegend), TIM4 (PerCy5.5, clone RMT4-54, Thermo Scientific). IFN-γ (PE, clone XMG1.2, BD Biosciences) and Ki67 (PE, BD Biosciences) were detected after intracellular staining according to the manufacturer's protocol. Isotype-matched control monoclonal antibodies were used to ensure the specificity of the stainings. Stained cells were analysed on a FACS Canto II cytometer or on a Spectral Aurora cytometer. Flow cytometry data were analysed with FlowJo v10 (Treestar) or Cytek Spectroflow software. For the osteopontin intracellular (Alexa fluor 647) staining, we used the Prime Flow RNA assay (Life technology, 88–18 005-210 and PF-210, ASSAY ID VB1-14709-PF) according to the manufacturer's protocol.

2.5 | SCENITH

The liver isolated non-parenchymal fraction (NPF) was stimulated for 5 h with LPS (1 μg/mL). Then the cells were washed with PBS and incubated with different metabolic inhibitors (deoxyglucose (DG), Oligomycin (O) or deoxyglucose + oligomycin (DGO)). After 15 min, puromycin was added for 30 min. After the incubation period, the cells were washed with PBS and kept ready for flow cytometry staining. NK cells were targeted with the extracellular markers NKp46 and CD49b among CD45^{+} cells. Finally, intracellular staining was performed to detect puromycin incorporation into the cells with anti-puro Alexafluor647 antibody (MERCK). Labelled cells were analysed on FACS Canto II cytometer. Flow cytometry data were analysed with FlowJo v10 software (Treestar).

2.6 | NK Cell Expansion

Liver NK cells suspension was labelled with biotinylated antibodies against non-NK cell lineage, and the unlabelled cell fraction was enriched using Rapidspheres (StemCell Technologies), following the manufacturer's instructions. Isolated NK cells

were expanded for 10 days in RPMI medium (supplemented with 10% SVF, Pen/Strep, L-Glutamine, pyruvate sodium and β-Mercaptoethanol) with IL15 (100 ng/mL). Every 4 days, a survival dose of IL15 (10 ng/mL) was added.

2.7 | Liver NK Cells Stimulation

Expanded NK cells (1.10^6) were then stimulated with 1 μg/mL of LPS (Sigma) or with IL12 (20 ng/mL, Tocris) + IL18 (5 ng/mL, Tocris). The supernatant of LPS-stimulated NK cells was kept for hepatocyte stimulation, and the cells were then washed with PBS, and the pellet frozen until RNA extraction (RNeasy Mini Kit, Qiagen).

2.8 | Primary Hepatocyte and Bone Marrow-Derived Macrophages Stimulation

As we previously described in Luci et al. [29], mouse hepatocytes were isolated with a two-step collagenase procedure. The cell suspension was then filtered and hepatocytes were pelleted after 2 centrifugations at 50 g for 5 min. Pelleted hepatocytes were resuspended in 40% Percoll solution, centrifuged at 50 g for 5 min at room temperature and collected at the bottom of the tube. For cell adhesion, primary hepatocyte were cultured during 24 h in William's E medium. Then the supernatant was removed and the primary hepatocyte were stimulated during 24 h with the supernatant of NK cells stimulated or not with LPS. Bone marrow macrophages were prepared as previously described [29] and stimulated during 24 h with the supernatant of NK cells stimulated or not with LPS. The supernatant is kept for ELISA assay and the cells were then washed with PBS and frozen until ARN extraction (RNeasy Mini Kit, Qiagen).

2.9 | ELISA Assay

For cytokine determination, culture supernatants were analysed by ELISA assay kits for murine: IFNγ, IL6, TNFα, CXCL10 (R&D system) according to the manufacturer's instructions.

2.10 | Real-Time Quantitative PCR Analysis

Total liver RNA was extracted using the RNeasy Mini Kit (74 104, Qiagen, Hiden, Germany) and treated with Turbo DNA-free (AM 1907, Thermo Fisher Scientific Inc.) following the manufacturer's protocol. The quality and quantity of the RNA were determined using the Agilent 2100 Bioanalyzer with RNA 6000 Nano Kit (5067–1511, Agilent Technologies, Santa Clara, CA, USA). Total RNA (1 μg) was reverse-transcribed with High-Capacity cDNA Reverse Transcription Kit (Thermo Fisher Scientific Inc.). Real-time quantitative PCR was performed in duplicate for each sample using StepOne plus Real-Time PCR system (Thermo Fisher Scientific Inc.), as previously described [29]. Gene expression was normalised to the housekeeping gene RPLP0 (Ribosomal Phosphoprotein Large P0 Mouse) and calculated based on the comparative cycle threshold Ct method ($2^{-\Delta\Delta Ct}$).

2.11 | TaqMan Gene Expression Assay

Mouse TaqMan gene expression assays were purchased from ThermoFisher Scientific Inc.: *B2m* (Mm00437762_m1), Rplp0 (Mm99999223_gH), *Timp1* (Mm00441818_m1), *Col1a1* (Mm00801666_g1), *Ccl2* (Mm00441242_m1), *Itgax* (*Cd11c*, Mm00498698_m1), *Itgam* (*Cd11b*, Mm01271265_m1), *Cd44* (Mm01277163_m1), *Spp1* (Osteopontin, Mm01611440_mH), *Tgfb* (Mm03024053_m1), *Tnfa* (Mm00443258_m), *Csf2* (Mm99999059_m1), *Ifng* (Mm01168134_m1), *Il6* (Mm00446190_m1), *Cxcl1* (Mm00433859_m1). Human TaqMan assays were also purchased from ThermoFisher Scientific Inc.: *Eomesodermin* (Hs00172872_m1), *Cd44* (Hs00153304_m1).

2.12 | Histology

Liver and gut tissue was fixed in 10% buffered formalin, embedded in paraffin, sectioned (5 μm thick) and stained with either haematoxylin and eosin (H/E) or Sirius red. Specimens were evaluated under a light microscope with a charge-coupled device camera (Nikon) and transferred to a TV monitor on the C3M Imaging facility (part of Microscopy and Imaging platform Côte d'Azur, MICA). Histopathological features were observed, such as steatosis (lipid droplets quantification) and inflammatory foci numeration in the liver. Fibrosis (percentage of collagen positive area among total tissue section area) was quantified by polarised light analysis of tissue sections.

2.13 | Statistical Analysis

Statistical significance was assessed using Prism software version 7.0 (GraphPad Prism, San Diego, CA, USA). Depending on the data distribution, we used a Mann–Whitney test or pairwise multiple comparisons using two-way ANOVA with Benjamini correction. Correlations were analysed using the Spearman's correlation test.

3 | Results

3.1 | CD44 Deficiency in NKp46$^+$ ILCs Negatively Affects Liver CD49b$^+$ NK Cell and CD49a$^+$ ILC1 Numbers

As we previously reported that CD44 is a key actor of steatohepatitis by regulating the liver mobilisation and activity of myeloid cells in a context of MASLD and alcohol-related liver disease (ALD) [17, 18], we investigated whether CD44 could also influence the behaviour of NKp46$^+$ ILCs. Liver NK cells and ILC1s were identified as CD49b$^+$ CD49a$^-$ cells and CD49b$^-$ CD49a$^+$ cells, respectively. As previously described, hepatic expression of the transcription factor eomesodermin helps to distinguish CD49b$^+$ CD49a$^-$ NK cells from CD49b$^-$ CD49a$^+$ ILC1s. NK cells and ILC1s also share expression of cell surface receptors such as NKG2A, NKG2D and

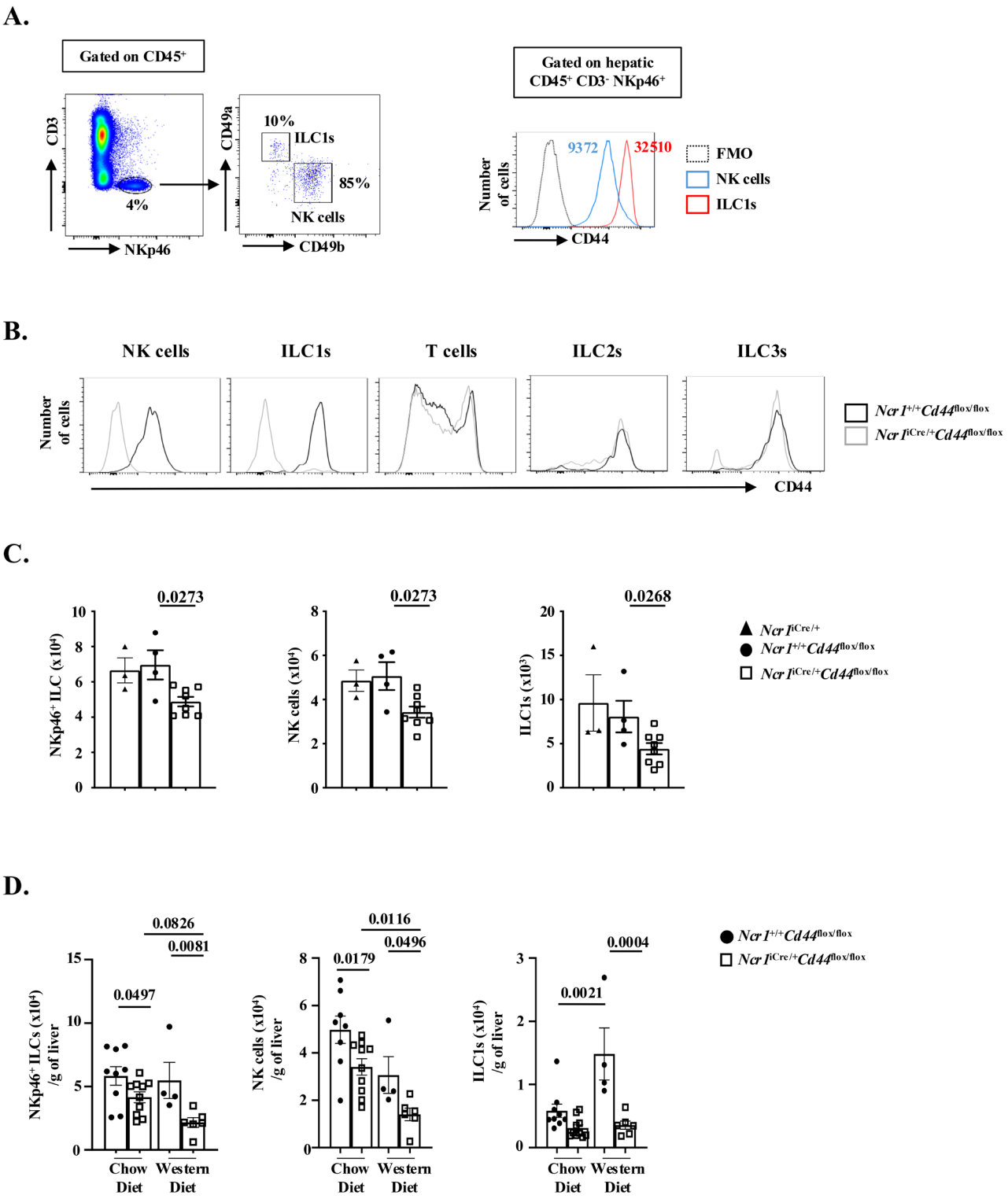

FIGURE 1 | CD44 deficiency in NKp46$^+$ ILCs affects liver NK cell and ILC1 numbers. (A) Representative flow cytometry dot plots showing frequencies of liver CD49a$^+$ ILC1s and CD49b$^+$ NK cells after gating on CD45$^+$ CD3$^-$ NKp46$^+$ cells from WT naive mice (left panel). Representative histogram plots showing cell surface expression of CD44 on liver CD49a$^+$ ILC1s (red line) and CD49b$^+$ NK cells (blue line) after gating on hepatic CD45$^+$ CD3$^-$ NKp46$^+$ cells from WT naive mice. Numbers indicate mean fluorescence intensity. FMO: Fluorescence minus one + isotype control antibody (black dotted line) (right panel). (B) Representative histogram plots showing the expression level of CD44 in liver NK cells, ILC1s, ILC2s, ILC3s, and T cells of naive NKp46$^{iCre/+}$CD44$^{flox/flox}$ mice compared to naive NKp46$^{+/+}$CD44$^{flox/flox}$ and NKp46$^{iCre/+}$ littermate mice. (C) Number of NKp46$^+$ ILCs, NK cells, and ILC1s evaluated by flow cytometry in livers of NKp46$^{+/+}$CD44$^{flox/flox}$ and NKp46$^{iCre/+}$CD44$^{flox/flox}$ under a chow diet. (D) NKp46$^+$ ILC, NK cell, and ILC1 number evaluated by flow cytometry in livers of NKp46$^{+/+}$CD44$^{flox/flox}$ and NKp46$^{iCre/+}$CD44$^{flox/flox}$ mice fed for 24 weeks with chow diet or Western diet. Histograms represent mean values ± SEM of pooled data from 2 to 3 independent experiments ($n = 4–10$ mice/group). p values are indicated for two-way ANOVA analysis with Benjamini correction. Statistical significance was defined as $p < 0.05$.

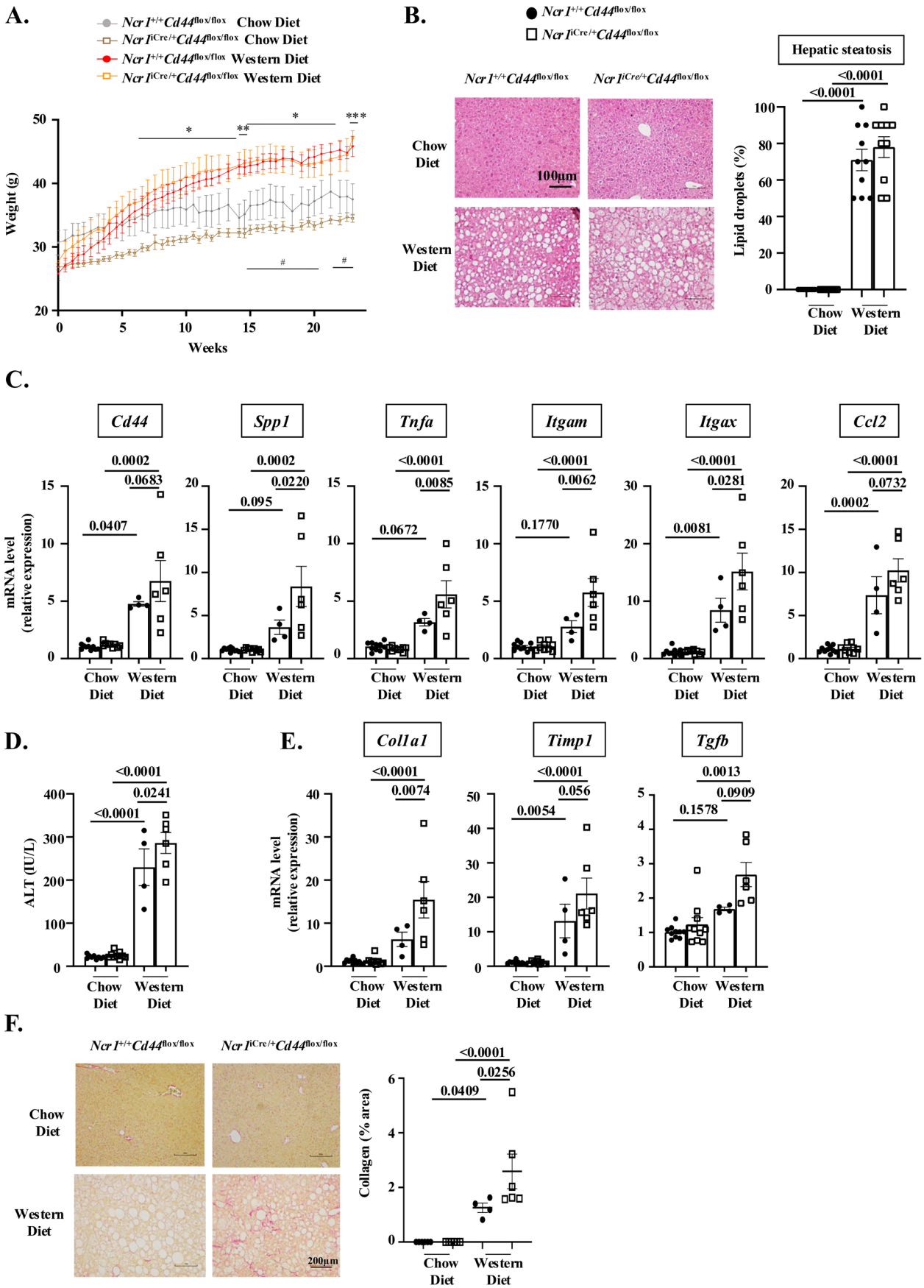

FIGURE 2 | Legend on next page.

FIGURE 2 | CD44 deficiency in NKp46$^+$ ILCs aggravates liver abnormalities after 24 weeks on Western Diet. (A) Body weight monitoring of NKp46$^{+/+}$CD44$^{flox/flox}$ and NKp46$^{iCre/+}$CD44$^{flox/flox}$ mice fed with chow diet or Western diet for 24 weeks. Statistics correspond to the comparison between Ncr1$^{iCre/+}$ CD44$^{flox/flox}$ mice challenged with WD versus Ncr1$^{icre/+}$ CD44$^{flox/flox}$ mice challenged with CD (*) and Ncr1$^{+/+}$ CD44$^{flox/flox}$ mice challenged with WD versus Ncr1$^{+/+}$ CD44$^{flox/flox}$ mice challenged with CD ($^{\#}$). (B) Haematoxylin and Eosin (H&E) staining of liver tissue sections and quantification of hepatic steatosis. (C) Hepatic mRNA expression levels of inflammatory associated markers evaluated by real-time quantitative PCR. (D) Serum level of ALT activity. (E) Hepatic mRNA expression levels of fibrotic genes. (F) Representative Sirius red staining of liver tissue sections (left panel) and quantification of collagen area in tissue sections (right panel). All real-time quantitative PCR data are presented as relative mRNA expression levels normalised to the *β2M* mRNA level. Histograms represent mean ± SEM of pooled data from 2 independent experiments ($n = 4$–10 mice/group). p values are indicated for two-way ANOVA analysis with Benjamini correction. Statistical significance was defined as $p < 0.05$. $^*p < 0.05$, $^{**}p < 0.001$, $p < 0.0001$,$^{\#}p < 0.05$.

produce IFN-γ, whereas KLRG1 and CD69 are preferentially expressed by NK cells and ILC1, respectively (Figure S1). We confirmed that NK cells and ILC1s expressed CD44, with a higher expression in ILC1s as previously reported (Figure 1A) [30, 31]. To address the role of CD44 in NKp46$^+$ ILCs' physiology, we deleted *Cd44* in NKp46-expressing cells by crossing *Cd44*$^{flox/flox}$ mice with *Ncr1*$^{iCre/+}$ mice. As expected, liver NK cells and ILC1s failed to express CD44, while its expression remained unaltered in T cells, ILC2s and ILC3s in *Ncr1*$^{iCre/+}$*Cd44*$^{flox/flox}$ mice compared to their littermate *Ncr1*$^{+/+}$*Cd44*$^{flox/flox}$ counterparts (Figure 1B). This specific deficiency was also sufficient to decrease the absolute number of hepatic NKp46$^+$ ILCs, NK cells and ILC1s on a chow diet (Figure 1C). These results indicate that our new mouse model of CD44 deficiency in NK cells and ILC1s represents a reliable model to study their contribution in chronic liver diseases.

3.2 | CD44 Deficiency in NKp46$^+$ ILCs Aggravates Liver Abnormalities Upon Western Diet Feeding

To evaluate the impact of CD44 deficiency in NK cells and ILC1s on liver diseases, we fed our knockout mice a Western Diet (WD) that promotes the development of obesity and MASLD. As in naive mice (Figure 1A), CD49b and CD49a were similarly expressed by NK cells and ILC1, respectively (Figure S2A). The analysis of the dynamics of liver NK cells and ILC1s indicated that although the total number of NKp46$^+$ ILCs per g of liver was identical between control diet mice and WD-fed mice, the number of ILC1s was increased in littermate *Ncr1*$^{+/+}$*Cd44*$^{flox/flox}$ mice challenged with Western Diet (Figure 1D and Figure S2B). In *Ncr1*$^{iCre/+}$*Cd44*$^{flox/flox}$ mice fed with Western Diet, we found a reduced number of NKp46$^+$ ILCs, ILC1s, and NK cells compared to littermate *Ncr1*$^{+/+}$*Cd44*$^{flox/flox}$ mice, as observed in chow diet (Figure 1D). This discrepancy was not associated with any difference in WD-induced weight gain between the two genotypes (Figure 2A). Next, we assessed the impact of these changes on the development of liver disease. Both genotypes developed hepatic steatosis to a similar extent after 24 weeks of WD (Figure 2B). However, we observed an aggravation of hepatic inflammation in WD-challenged *Ncr1*$^{iCre/+}$*Cd44*$^{flox/flox}$ mice compared to littermate mice, as evidenced by increased gene expression of inflammatory markers *Spp1* (encoding osteopontin, one of the CD44 ligands), *Itgam* (encoding for CD11b), *Itgax* (encoding for CD11c) and *Tnfa*, while *Cd44* and *Ccl2* expression also tended to increase (Figure 2C). This exacerbation of liver inflammation was also associated with greater liver injury (as evaluated by higher ALT activity levels) (Figure 2D) and hepatic fibrosis, as evidenced by augmented expression of the pro-fibrogenic marker *Col1a1* and collagen deposits, while *Timp1* and *Tgfb* expression also tended to increase (Figure 2E,F). Collectively, these data highlight the tight regulation of steatohepatitis by CD44-expressing NKp46$^+$ ILCs.

3.3 | CD44 Deficiency in NKp46$^+$ ILCs Aggravates Liver Abnormalities in Response to Methionine and Choline Deficient Diet-Induced Steatohepatitis

We next investigated whether the absence of CD44 in NKp46$^+$ ILCs could also accelerate the progression of liver complications in a context of methionine and choline deficiency. It has been well established that the methionine and choline deficient diet rapidly induces severe liver injury and inflammation. These local complications are independent of obesity and insulin resistance. After 4 weeks of MCDD feeding, we observed an increased number of hepatic NKp46$^+$ ILCs and NK cells in littermate mice as previously reported for wild-type mice (Figure 3A) [14, 32]. Further, *Ncr1*$^{iCre/+}$*Cd44*$^{flox/flox}$ mice displayed a significant reduction in the absolute number of NKp46$^+$ILCs, NK cells and ILC1s after 4 weeks of MCDD compared to *Ncr1*$^{iCre/+}$*Cd44*$^{flox/flox}$ mice (Figure 3A). This reduction was likely due to CD4's role in proliferation control rather than a defect in circulating cell recruitment, as Ki67 staining, evaluated by flow cytometry, was decreased in NK cells from MCDD-fed *Ncr1*$^{iCre/+}$*Cd44*$^{flox/flox}$ mice, while the CXCR3/CXCL10 axis was unaffected (Figures 3B and S3). Histological analyses did not reveal any difference in hepatic steatosis in MCDD-fed *Ncr1*$^{iCre/+}$*Cd44*$^{flox/flox}$ mice compared to MCDD-fed littermate mice (Figure 3C). Similarly to the WD mouse model, the absence of CD44 in NKp46$^+$ ILCs aggravated liver inflammation and injury (as evaluated by the expression of inflammatory markers and ALT activity, respectively) (Figure 3D,E), as well as liver fibrosis (as evaluated by fibrotic marker expressions and collagen deposits) (Figure 3F,G). Furthermore, we also showed that IFN-γ production was augmented in NK cells from *Ncr1*$^{iCre/+}$*Cd44*$^{flox/flox}$ mice fed a MCDD, with preferential increase in their glycolytic capacity at the expense of oxidative phosphorylation, as evaluated by flow cytometry and the SCENITH method (Figure 4A,B) [33].

We next investigated whether such increased liver inflammation observed in MCDD-fed *Ncr1*$^{iCre/+}$*Cd44*$^{flox/flox}$ mice was associated with changes in the composition of hepatic macrophage subsets known to participate in MASH pathogenesis. In line with this, the number of F4/80$^+$ CD11b^{high} CD11c$^+$ inflammatory macrophages and CLEC2$^-$ TIM4$^-$ Osteopontin$^+$ macrophages, a subset of recruited macrophages termed LAMs (Lipid-associated macrophages) that replace resident Kupffer

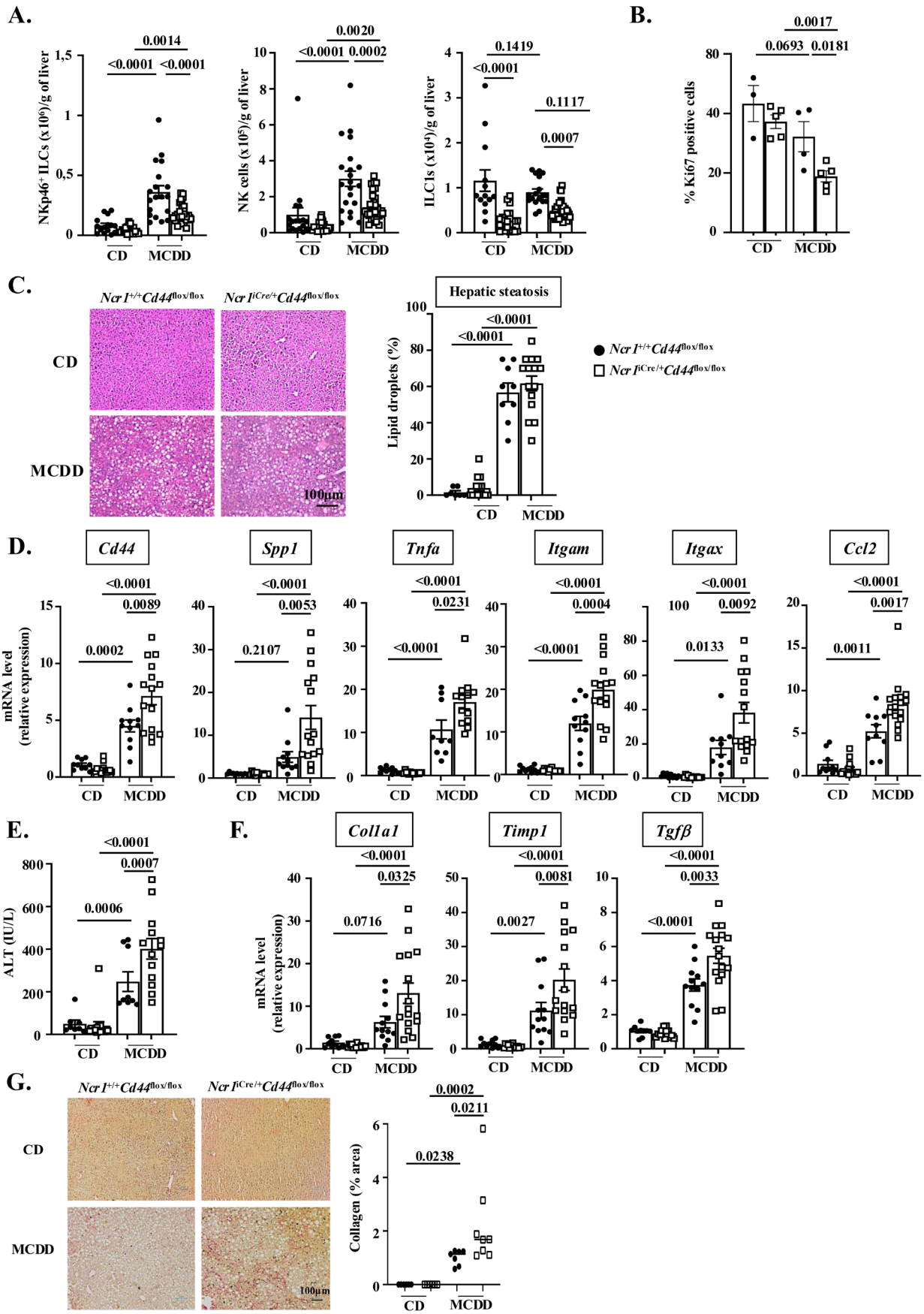

FIGURE 3 | Legend on next page.

FIGURE 3 | CD44 deficiency in NKp46^{+} ILCs aggravates liver abnormalities after 4 weeks of Methionine and Choline Deficient Diet. (A) NKp46^{+} ILC, NK cell and ILC1 number evaluated by flow cytometry in livers of NKp46$^{+/+}$CD44$^{flox/flox}$ and NKp46$^{iCre/+}$CD44$^{flox/flox}$ mice fed for 4 weeks with control diet (CD) or Methionine and Choline Deficient Diet (MCDD). (B) Ki67 staining evaluated by flow cytometry. (C) Haematoxylin and Eosin (H & E) staining of liver tissue sections and quantification of hepatic steatosis. (D) Hepatic mRNA expression levels of inflammatory associated-markers evaluated by real-time quantitative PCR. (E) Serum level of ALT activity. (F) Hepatic mRNA expression levels of fibrotic genes. (G) Representative Sirius red staining of liver tissue sections (left panel) and quantification of collagen area in tissue sections (right panel) in livers of NKp46$^{+/+}$CD44$^{flox/flox}$ and NKp46$^{iCre/+}$CD44$^{flox/flox}$ mice. All real-time quantitative PCR data are presented as relative mRNA expression levels normalised to the *β2M* mRNA level. Histograms represent mean values ± SEM of pooled data from 2 to 4 independent experiments ($n = 8$–19 mice/group). *p* values are indicated for two-way ANOVA analysis with Benjamini correction. Statistical significance was defined as $p < 0.05$.

cells during MASH [17, 34] was increased in the livers of MCCD-challenged mice, with a more pronounced infiltration in *Ncr1*$^{iCre/+}$*Cd44*$^{flox/flox}$ mice (Figure 4C,D). In addition, after WD feeding, the absence of CD44 in NKp46 cells is also associated with the increased recruitment of CLEC2^{-} TIM4^{-} osteopontin^{+} macrophages to the liver as found upon MCDD challenge (Figure S4). Overall, the MCDD mouse model reinforces the results obtained with the WD model in the regulation of liver inflammation by CD44-expressing hepatic ILCs.

3.4 | The Lack of CD44 Predisposes the NK Cells to an Inflammatory Phenotype in Response to LPS

This aggravation of liver inflammation could be caused by the overactivity of CD44-deficient NK cells. It has been well established that PAMPs, including LPS, are major regulators of hepatic immune cell activation and sustained liver inflammation. First, we verified that liver NK cells express TLR4 by qPCR and by analysing a public database (Figure S5A). Next, we exposed enriched liver NK cells to LPS in vitro and we analysed metabolic pathways, as well as cytokine and chemokine profiles (Figures 5A and S5B). We confirmed our in vivo data showing that liver CD44-deficient NK cells preferentially increase their glycolytic capacity in response to LPS at the expense of oxidative phosphorylation (Figure 5B). To further evaluate the activity of the CD44-deficient NK cells, we assessed their cytokine and chemokine profiles. Enriched LPS-treated CD44-deficient NK cells showed significantly higher expression of pro-inflammatory mediators including *Ifng*, *Csf2* (GM-CSF) and *Il6* compared to CD44-sufficient NK cells (Figure 5C,D, respectively). We confirmed that IFN-γ production is significantly higher in LPS-treated CD44-deficient NK cells by ELISA (Figure 5C). Further, CD44 does not regulate IFNγ, TNFα and GM-CSF production after stimulation with IL12 + IL18 (Figure S5C). Taken together, these findings suggest that CD44-deficient NK cells are more sensitive to LPS and could contribute to the aggravation of hepatic necro-inflammation.

3.5 | The Inflammatory Phenotype of CD44-Deficient NK Cells Enhances Production of Pro-Inflammatory Mediators by Hepatocytes and Macrophages

To validate that CD44-deficient NK cells contribute to the local inflammation and liver damage during steatohepatitis, we then investigated the direct effect of cytokines derived from LPS-treated NK cells on hepatocytes and macrophages in vitro (Figures 6A and 7A, respectively). Primary hepatocytes and bone marrow macrophages isolated from healthy mice were treated with the supernatant of LPS-treated CD44-deficient NK cells (Sup$^{NK\text{-}CD44KO}$) or LPS-treated CD44-sufficient NK cells (Sup$^{NK\text{-}WT}$). We showed that LPS-Sup$^{NK\text{-}CD44KO}$ treatment increased the expression of pro-inflammatory mediators including *Tnfa*, *Il6* and *Cxcl1* in primary hepatocytes and bone marrow macrophages (Figures 6B and 7B), and oxidative stress markers, including *nos2* and *gp91phox*, in primary hepatocytes (Figure 6B). To note, the treatment of hepatocytes with LPS alone did not significantly increase the expression of these markers (Figure 6B). In addition, the secretion of the pro-inflammatory factors TNF-α, IL-6, and CCL2 by primary hepatocytes was enhanced in response to LPS-Sup$^{NK\text{-}CD44KO}$ conditioned medium (Figure 6C). Collectively, these results suggest that CD44 is a novel regulator of LPS-dependent NK cell responses. Its absence in NK cells may contribute to the aggravation of local inflammation by amplifying the expression of pro-inflammatory mediators by NK cells, which in turn increase the release of additional inflammatory mediators by hepatocytes and macrophages, thereby favouring the progression of steatohepatitis.

3.6 | Hepatic NK Cell Marker Is Associated With MASLD Features in Patients With Obesity

We then examined Cd44 and Eomesodermin expression, which helps to define also human hepatic NK cells, in human liver cells and their relationship to MASLD [35]. From Gene Expression Omnibus public database under accession number GSE192742, liver resident NK cells displayed an elevated expression level of Cd44 and Eomesodermin (Figure 6A) [36]. We also analysed hepatic expression of Cd44 and Eomesodermin in liver biopsies from patients with severe obesity who had undergone bariatric surgery. Patients were classified into 2 groups: without MASLD ($n = 7$) and with MASLD ($n = 13$), including 8 patients with hepatic steatosis and 5 with steatohepatitis (based on histopathological features; Table S1). Hepatic expression of Cd44 and Eomesodermin was upregulated at the mRNA level in MASLD patients (Figure S6B). The upregulation of Eomesodermin also correlated with the hepatic expression of Cd44 (Figure S6C). These results indicate that NK cells may also be involved in the development of liver complications in patients with obesity.

4 | Discussion

It is now well established that chronic inflammation and activation of innate immune cells are essential features of MASLD. A

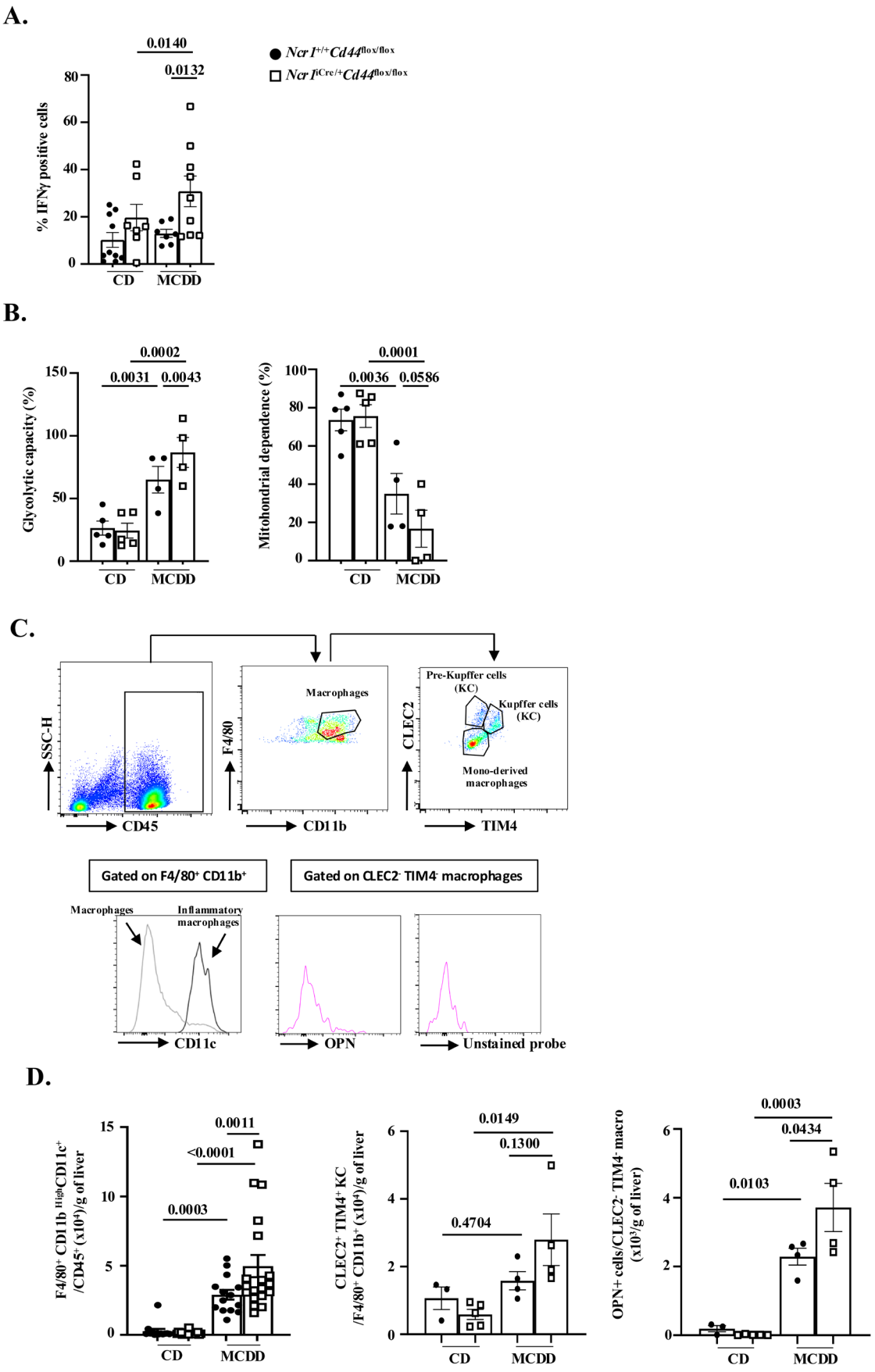

FIGURE 4 | Legend on next page.

FIGURE 4 | CD44 deficiency in NKp46$^+$ ILCs enhances NK cell functions and regulates liver macrophage subsets after 4 weeks of Methionine and Choline Deficient Diet. (A) IFN-γ production by NK cells evaluated by flow cytometry in livers of NKp46$^{+/+}$CD44$^{flox/flox}$ and NKp46$^{iCre/+}$CD44$^{flox/flox}$ mice fed for 4 weeks with control diet (CD) or Methionine and Choline Deficient Diet (MCDD). (B) Determination of NK cell glycolytic capacity and mitochondrial dependence measured by Scenith experiment. (C) Representative flow cytometry gating strategy of liver cells allowing identification of liver macrophage subsets. (D) Hepatic frequencies of liver macrophage subsets determined by flow cytometry in NKp46+/+CD44flox/flox and NKp46iCre/+CD44flox/flox mice fed with CD or MCDD. Histograms represent mean values ± SEM of pooled data from 2 to 3 experiments (3–19 mice/group). *p* values are indicated for two-way ANOVA analysis with Benjamini correction. Statistical significance was defined as $p < 0.05$.

growing body of evidence indicates that innate lymphoid cells and, in particular, NK cells and ILC1s are important players in steatohepatitis pathogenesis [3, 37]. In this study, we demonstrate that steatohepatitis is associated with increased hepatic NKp46$^+$ ILC numbers in murine dietary models of MASH and steatohepatitis. We show that CD44 regulates the abundance of NKp46$^+$ ILCs in liver tissue presumably by regulating their proliferation. Furthermore, the specific deletion of CD44 within NKp46$^+$ ILCs aggravates liver inflammation and injury, as well as liver fibrosis, notably through the establishment of an inflammatory loop with hepatocytes and macrophages.

Our study reports that livers of CD44-deficient NKp46$^+$ ILCs mice fed with MASH diets express higher levels of markers of macrophage recruitment/activation (*cd11b*, *cd11c*, *ccl2*, *cd44*, *spp1*). CD44 and osteopontin (*spp1*) are reliable markers of liver macrophages participating in MASH pathogenesis [17, 34]. Hepatic macrophage infiltration has been described in mouse dietary models of MASLD (high-fat diet (HFD) and MCDD) [34, 38–40]. The liver is comprised of liver-resident Kupffer cells (KC) and recruited monocyte-derived macrophages. It has been proposed that KC are the first responders upon liver injury, secreting proinflammatory mediators such as TNF-α, CCL2, CXCL10 and in turn leading to recruitment of monocyte-derived macrophages and NK cells [32, 38, 41]. An elegant study accurately characterised the origin and dynamics of the distinct liver macrophage subsets in MASH using the KC-specific markers Clec4F and Timp4. In MASH liver, the KC pool is maintained by proliferation and differentiation of short-lived monocyte-derived KC, presumably due to increased pro-inflammatory mediators in the liver environment [42, 43]. Further, monocytes recruited to the liver also differentiated into a distinct subset of osteopontin-expressing CLEC2$^-$ macrophages that contribute to MASH disease [40]. In line with this, we found that *Ncr1*$^{iCre/+}$*Cd44*$^{flox/flox}$ mice displayed a higher frequency of F4/80$^+$ CD11b^{high} CD11c$^+$ inflammatory macrophages and CLEC2$^-$ TIM4$^-$ Osteopontin$^+$ macrophages upon WD or MCCD challenge.

Liver NK cell-derived IFNγ is also an important contributor to the polarisation of pro-inflammatory macrophages, which in turn sustain liver inflammation [14]. We also report that IFN-γ production by LPS-treated NK cells was strongly increased when CD44 is absent, suggesting a potential role of NK cells expressing CD44 in regulating liver IFN-γ levels and macrophage polarisation. The role of IFN-γ in macrophage activation is well known, notably through the induction of pro-inflammatory cytokine secretions such as TNF-α or IL-1β [44]. However, its mechanism in the MASH context is still debated, and IFN-γ seems to be more specifically involved in the priming of macrophages. IFN-γ could induce internal changes within macrophages, which could be responsible for the robust inflammatory response triggered by TLR ligands during macrophage activation [45, 46].

Regarding the direct role of LPS on NK cells, initial studies have demonstrated that human NK cells express the LPS receptors TLR2 and TLR4 at the gene level [47–49]. In line with our results, Kanevskiy et al. revealed that LPS had a stimulatory effect on IFN-γ production by human NK cells [50, 51]. Whether CD44 and LPS receptors form a complex at the cell surface of NK cells to trigger IFN-γ production still deserves further investigations. Interestingly, as demonstrated in the work of Freeman et al. [52], we assume that CD44 can associate indirectly with F-actin, suggesting it may function as a membrane picket. It transiently anchors to formin-induced actin filaments, thereby limiting the lateral diffusion of surface receptors and facilitating activation of intracellular pathways for migration and/or cytokine production. In the context of acute liver injury, liver sinusoidal endothelial cells (LSECs) activated by LPS are important sources of myeloid cell-attracting chemokines such as CCL2 and CXCL10, which support NK cell recruitment and IFN-γ production [53]. Hepatocytes, the predominant cells in the liver capable of detecting pathogens such as LPS, also contribute to the regulation of hepatic cytokines and chemokines, leading to the recruitment of inflammatory cells to the liver [29]. Interestingly, we report that isolated primary hepatocytes showed a huge increase in the expression of inflammatory and oxidative stress markers after stimulation with the supernatant of CD44-deficient NK cells activated with LPS. Our results are in line with a recent study showing that NK cells isolated from inflamed liver secrete pro-inflammatory cytokines able to activate the nuclear factor kappa B signalling pathway, responsible for the establishment of a significant inflammatory response by hepatocytes [54]. Further, this study proposed a promising protective role for ILC1 cells in addition to the pathogenic role for NK cells in fatty liver diseases using NK-cell and/or ILC1 deficient mice. We suggest that ILC1 may be protective in Western Diet of KO mice as the NK/ILC1 ratio decreased in WD compared to CD. The worsening of steatohepatitis observed in CD44-deficient NKp46$^+$ ILCs mice challenged with diet-induced steatohepatitis could thus be explained by a greater responsiveness of NK cells to LPS and the existence of a cross talk between NK cells, hepatocytes, and macrophages.

In our mouse model of genetic deletion of CD44 in NKp46$^+$ ILCs challenged with diet-induced steatohepatitis, we observed a marked elevation in liver fibrogenesis markers (*col1a1*, *timp1*, *tgfβ*) and collagen deposition associated with increased liver injury and inflammatory macrophages. The latter could overcome the anti-fibrogenic properties of NK cells recently reported in a mouse model of steatohepatitis [55]. Indeed, the NK cell depletion led to macrophage polarisation toward TGF-β producing

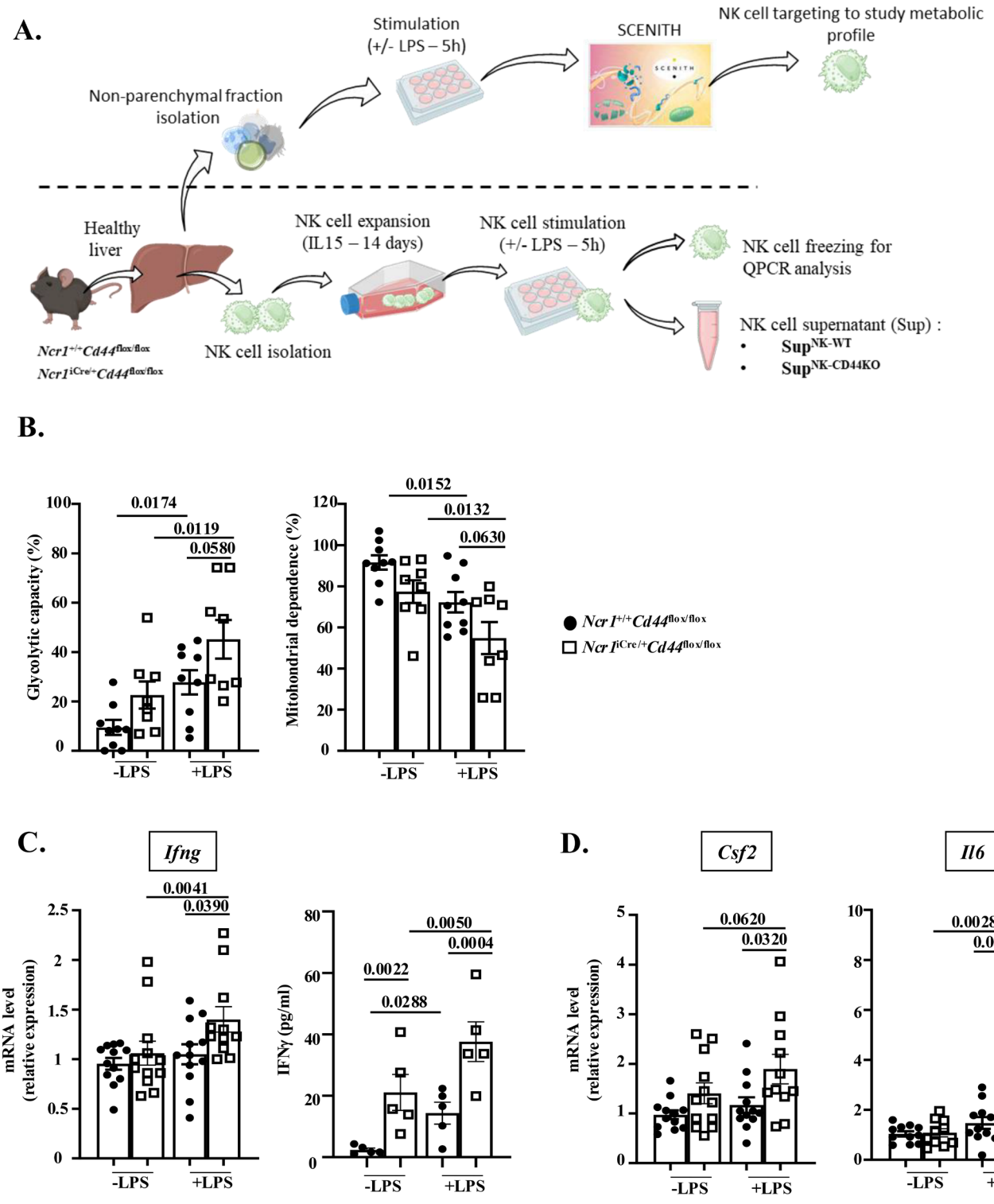

FIGURE 5 | The specific deficiency of CD44 in NK cells undergoes an increase in glycolytic capacity and inflammatory profile after LPS stimulation. (A) Schematic diagram for analysis of NK cell metabolism and derived cytokine produced after LPS stimulation. (B) Determination of NK cell glycolytic capacity and mitochondrial dependence measured by Scenith experiment after LPS stimulation (5 h, 1 μg/mL) of the non-parenchymal fraction of NKp46$^{+/+}$CD44$^{flox/flox}$ and NKp46$^{iCre/+}$CD44$^{flox/flox}$ mice. (C) NK cell mRNA expression of *Ifng* evaluated by real-time quantitative PCR and IFNg protein level measured by ELISA assay in the supernatant of NK cells stimulated with LPS (1 μg/mL) for 5 h. (D) NK cell mRNA expression of inflammatory-associated markers evaluated by real-time quantitative PCR. Real-time quantitative PCR data are presented as relative mRNA expression levels normalised to the *β2M* mRNA level. Histograms represent mean values ± SEM of pooled data from 2 to 3 independent experiments ($n = 5$–12 mice/group). *p* values are indicated for two-way ANOVA analysis with Benjamini correction. Statistical significance was defined as $p < 0.05$.

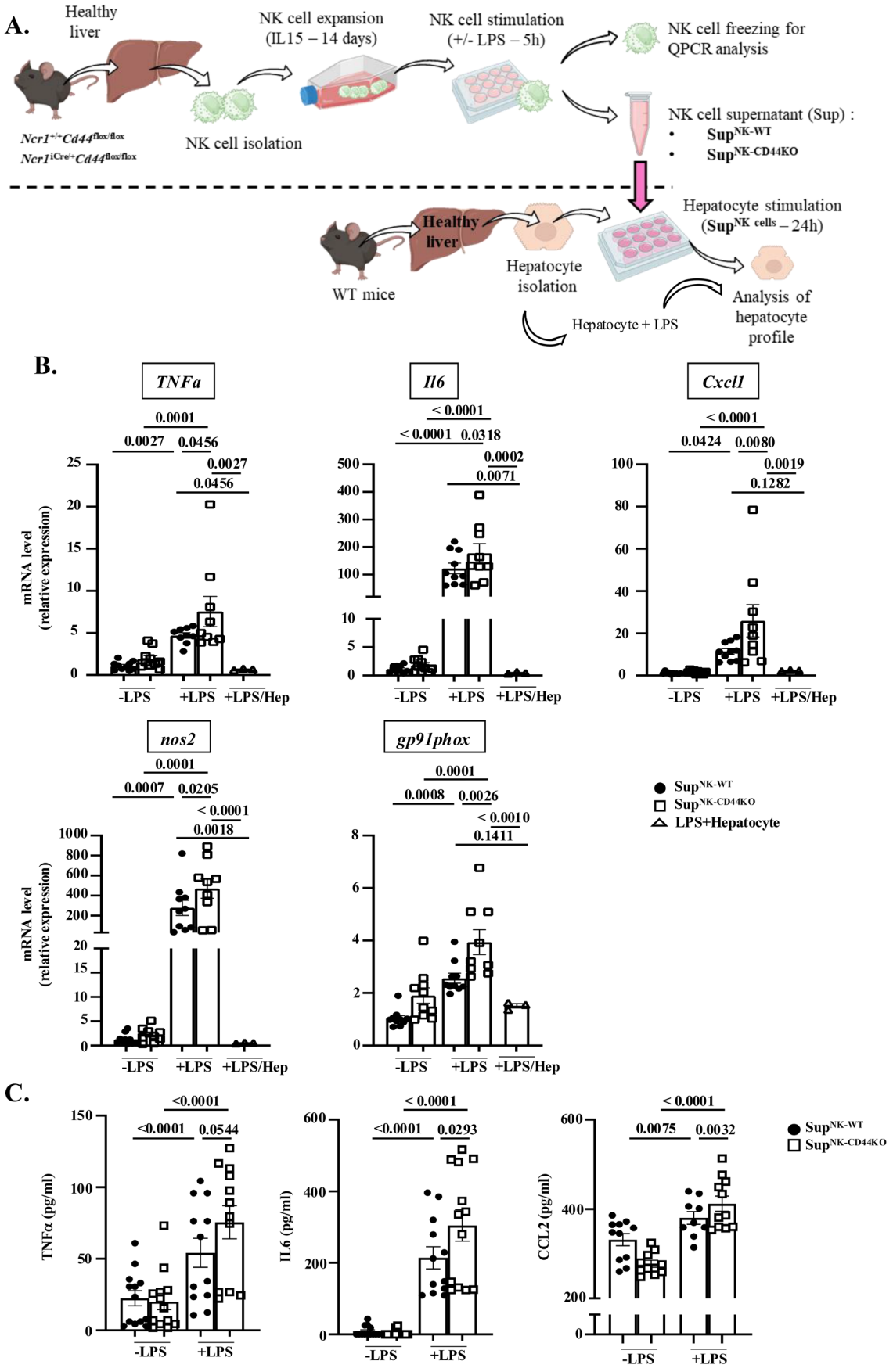

FIGURE 6 | Legend on next page.

FIGURE 6 | CD44-invalidated NK cells activated with LPS enhance the expression and the secretion of proinflammatory cytokines by primary hepatocytes. (A) Schematic diagram of NK cells derived supernatant treatment on hepatocytes. (B) Primary hepatocyte mRNA expression levels of inflammatory and oxidative stress markers after 24 h of stimulation with the supernatant of WT-NK cells and CD44-invalidated NK cells, activated with LPS or with LPS alone (LPS/Hep). Real-time quantitative PCR data are presented as relative mRNA expression levels normalised to the *Rplp0* mRNA level. (C) Cytokine levels measured by ELISA assay in the supernatant of primary hepatocytes after their stimulation. Histograms represent mean values ± SEM of pooled data from 3 independent experiments ($n = 9–13$ mice/group). *p* values are indicated for two-way ANOVA analysis with Benjamini correction. Statistical significance was defined as $p < 0.05$.

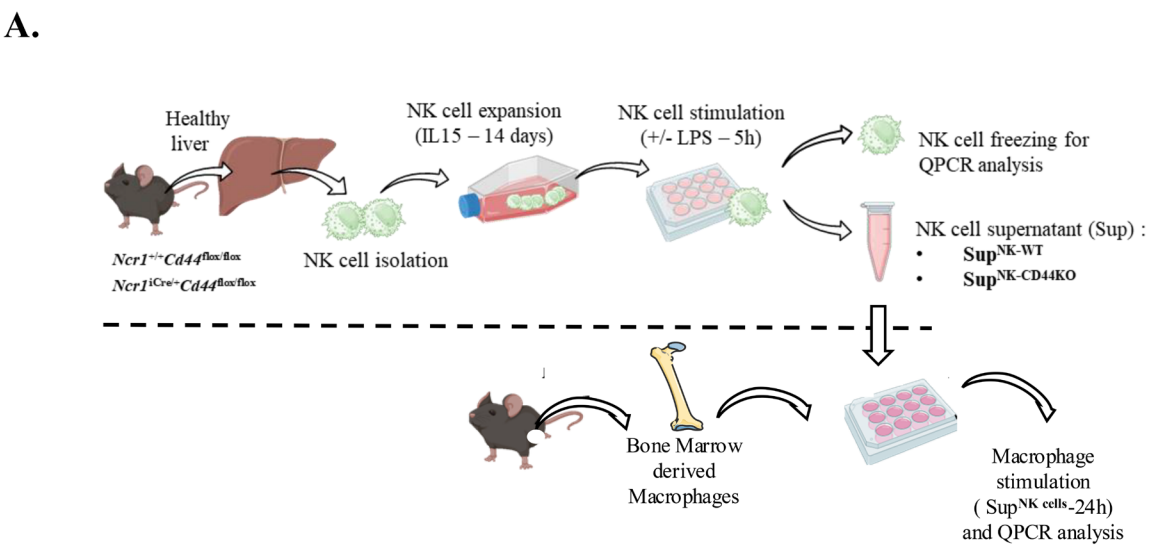

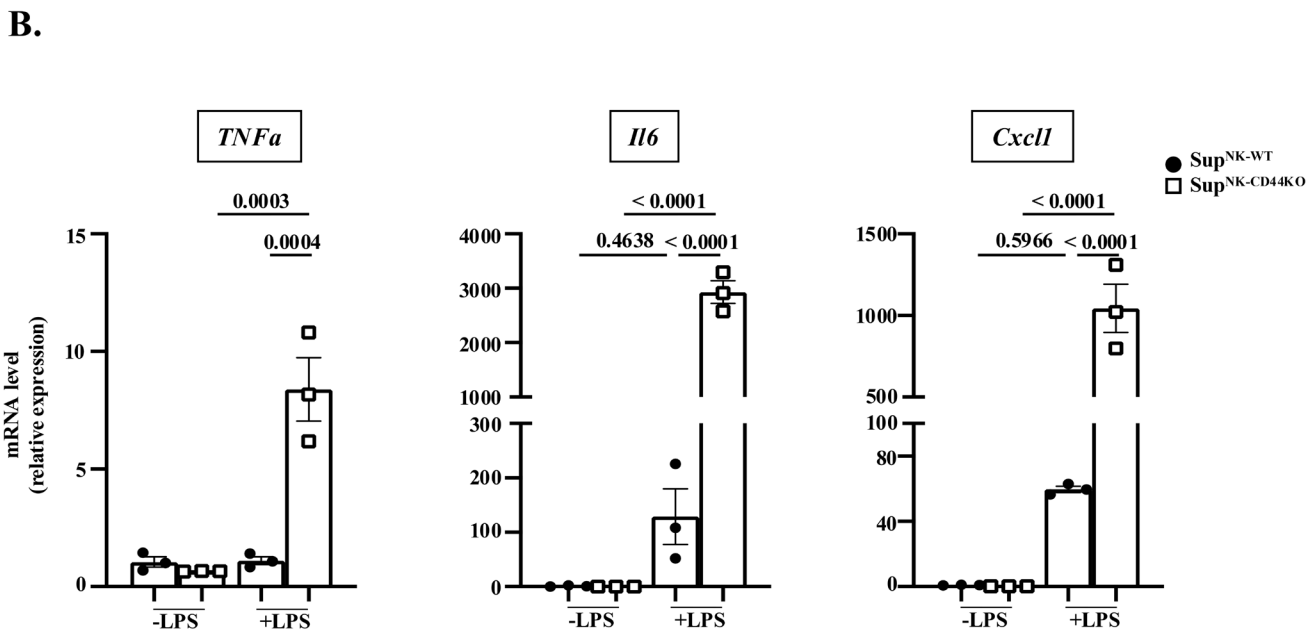

FIGURE 7 | CD44-invalidated NK cells activated with LPS enhance the expression and the secretion of proinflammatory cytokines by bone marrow-derived macrophages. (A) Schematic diagram of NK cells derived supernatant treatment on macrophages. (B) Primary macrophage mRNA expression levels after 24 h of stimulation with the supernatant of WT-NK cells and CD44-invalidated NK cells, activated with LPS. Real-time quantitative PCR data are presented as relative mRNA expression levels normalised to the *Rplp0* mRNA level. Histograms represent mean ± SEM of one experiment (three mice/group). *p* values are indicated for two-way ANOVA analysis with Benjamini correction. Statistical significance was defined as $p < 0.05$.

alternative macrophages which enhanced liver fibrosis [14]. Liver NK cells can also limit liver fibrosis by killing hepatic stellate cells (HSCs) via their cytotoxic activity. This mechanism is in part dependent on engagement of NK cell-activating receptors such as NKG2D and the TRAIL/TRAIL receptors pathway [55, 56]. Further, it has been proposed that the crosstalk between HSCs and NK cells is mediated through engagement of activating receptors NKp30, NKp46 or reduced engagement of inhibitory NK cell receptors [57, 58]. It will be interesting to assess the expression of activating receptors in CD44-deficient NK cells and their ability to recognise and kill HSCs to establish whether CD44 also regulates the anti-fibrogenic properties of NK cells. Our results also highlight that targeting CD44 as a therapeutic approach requires further in-depth study. We have previously reported that systemic targeting of CD44 by genetic deficiency and neutralisation prevents and corrects MASH and ALD, respectively. These approaches first affect cells that strongly express CD44 and are highly present in organs (macrophages, neutrophils) [17, 18]. Future investigations will be necessary to increase the specificity of the tools (targeting CD44 mainly in myeloid cells) and to adjust the dose and duration of treatment according to the results and side effects (targeting NK cells). In conclusion, we show that specific deletion of CD44 in NKp46^{+} ILCs represents a yet unknown mechanism of regulation of liver homeostasis during MASLD progression. Through our ex vivo approaches on NK cells, we have highlighted a potential role for CD44 in regulating LPS-mediated activation of NK cells. CD44-invalidated NK cells stimulated with LPS have their metabolic and functional activity increased, leading to the establishment of an inflammatory loop with hepatocytes. Finally, in the liver of patients with obesity and MASLD, expression of NK cell marker correlates with expression of CD44 and macrophage markers. Altogether, our study provides more insight into the pathogenesis of MASH/MASLD and should help to better understand the physiopathology of the disease.

Author Contributions

M.B. and E.V. performed the research and analysis and helped in editing the manuscript. D.R., S.B. performed the research and analysis. P.S.L., A.S., F.S., C.E., J.C.V., I.M. assisted with the experiments. S.P., A.I., R.A., A.T. contributed to human sample and data collection and provided intellectual insights. M.M., V.O.R. provided material support for the research and insights. M.K.T. A.B. assisted with experiments and helped in editing of the manuscript. B.B.M. provided insights. P.G. designed, supervised the research and wrote the manuscript. C.L. designed, supervised, performed, analysed the research, wrote, and edited the manuscript. All authors contributed to the manuscript and approved the submitted version.

Acknowledgements

The authors thank present and former members of Dr. Philippe Gual's laboratory for their helpful advice and suggestions, the C3M animal facilities and the cytometry platform. We are grateful to Pr. Eric Vivier (CIML, Innate Pharma, Marseille, France) for providing *Ncr1*^{iCre} mice, and Dr. Jeanne Tran-Van-Nhieu (CHU Henri Mondor, Department of Pathology, AP-HP—Université Paris Est Créteil, Créteil, France) for providing the liver samples from lean subjects. M.B., E.R., S.B., T.S., A.S., S.P., I.M., J.C.V., A.I., A.B., A.T., R.A., P.G., and C.L. also belong to the Adipo-Cible Research Study Group, at the Mediterranean Center for Molecular Medicine (C3M). We would also like to thank Catherine Buchanan for her assistance with English syntax and grammar in this manuscript.

Conflicts of Interest

Véronique Orlan-Rousseau consults for and owns stock in Amcure. The remaining authors have no conflicts to report.

Data Availability Statement

The data that support the findings of this study are available on request from the corresponding author. The data are not publicly available due to privacy or ethical restrictions.

References

1. M. E. Rinella, J. V. Lazarus, V. Ratziu, et al., "A Multisociety Delphi Consensus Statement on New Fatty Liver Disease Nomenclature," *Hepatology* 78 (2023): 1966–1986.

2. C. Luci, M. Bourinet, P. S. Leclere, R. Anty, and P. Gual, "Chronic Inflammation in Non-Alcoholic Steatohepatitis: Molecular Mechanisms and Therapeutic Strategies," *Frontiers in Endocrinology* 11 (2020): 597648.

3. M. Bourinet, R. Anty, P. Gual, and C. Luci, "Roles of Innate Lymphoid Cells in Metabolic and Alcohol-Associated Liver Diseases," *JHEP Reports: Innovation in Hepatology* 6 (2024): 100962.

4. A. D. Barrow and M. Colonna, "Innate Lymphoid Cell Sensing of Tissue Vitality," *Current Opinion in Immunology* 56 (2019): 82–93.

5. E. Vivier, D. Artis, M. Colonna, et al., "Innate Lymphoid Cells: 10 Years on," *Cell* 174 (2018): 1054–1066.

6. C. Luci, A. Reynders, I. I. Ivanov, et al., "Influence of the Transcription Factor RORgammat on the Development of NKp46+ Cell Populations in Gut and Skin," *Nature Immunology* 10 (2009): 75–82.

7. N. Satoh-Takayama, L. Dumoutier, S. Lesjean-Pottier, et al., "The Natural Cytotoxicity Receptor NKp46 Is Dispensable for IL-22-Mediated Innate Intestinal Immune Defense Against *Citrobacter rodentium*," *Journal of Immunology (Baltimore, Md: 1950)* 183 (2009): 6579–6587.

8. S. L. Sanos, V. L. Bui, A. Mortha, et al., "RORgammat and Commensal Microflora Are Required for the Differentiation of Mucosal Interleukin 22-Producing NKp46+ Cells," *Nature Immunology* 10 (2009): 83–91.

9. G. Gasteiger, X. Fan, S. Dikiy, S. Y. Lee, and A. Y. Rudensky, "Tissue Residency of Innate Lymphoid Cells in Lymphoid and Nonlymphoid Organs," *Science* 350 (2015): 981–985.

10. J. Cong, "Metabolism of Natural Killer Cells and Other Innate Lymphoid Cells," *Frontiers in Immunology* 11 (2020): 1989.

11. X. Michelet, L. Dyck, A. Hogan, et al., "Metabolic Reprogramming of Natural Killer Cells in Obesity Limits Antitumor Responses," *Nature Immunology* 19 (2018): 1330–1340.

12. E. Littwitz-Salomon, D. Moreira, J. N. Frost, et al., "Metabolic Requirements of NK Cells During the Acute Response Against Retroviral Infection," *Nature Communications* 12 (2021): 5376.

13. L. Riggan, A. G. Freud, and T. E. O'Sullivan, "True Detective: Unraveling Group 1 Innate Lymphocyte Heterogeneity," *Trends in Immunology* 40 (2019): 909–921.

14. A. C. Tosello-Trampont, P. Krueger, S. Narayanan, S. G. Landes, N. Leitinger, and Y. S. Hahn, "NKp46(+) Natural Killer Cells Attenuate Metabolism-Induced Hepatic Fibrosis by Regulating Macrophage Activation in Mice," *Hepatology* 63 (2016): 799–812.

15. E. Bourayou, T. Perchet, S. Meunier, et al., "Bone Marrow Monocytes Sustain NK Cell-Poiesis During Non-Alcoholic Steatohepatitis," *Cell Reports* 43 (2024): 113676.

16. A. R. Jordan, R. R. Racine, M. J. Hennig, and V. B. Lokeshwar, "The Role of CD44 in Disease Pathophysiology and Targeted Treatment," *Frontiers in Immunology* 6 (2015): 182.

17. S. Patouraux, D. Rousseau, S. Bonnafous, et al., "CD44 Is a Key Player in Non-Alcoholic Steatohepatitis," *Journal of Hepatology* 67 (2017): 328–338.

18. D. Rousseau, S. Bonnafous, F. Soysouvanh, et al., "CD44 in myEloid Cells Is a Major Driver of Liver Inflammation and Injury in Alcohol-Related Liver Disease," *Hepatology* (2025). doi:10.1097/HEP.0000000000001232

19. P. Johnson and B. Ruffell, "CD44 and Its Role in Inflammation and Inflammatory Diseases," *Inflammation & Allergy Drug Targets* 8 (2009): 208–220.

20. A. J. Ali, A. F. Abuelela, and J. S. Merzaban, "An Analysis of Trafficking Receptors Shows That CD44 and P-Selectin Glycoprotein Ligand-1 Collectively Control the Migration of Activated Human T-Cells," *Frontiers in Immunology* 8 (2017): 492.

21. J. D. Klement, A. V. Paschall, P. S. Redd, et al., "An Osteopontin/CD44 Immune Checkpoint Controls CD8+ T Cell Activation and Tumor Immune Evasion," *Journal of Clinical Investigation* 128 (2018): 5549–5560.

22. M. Qadri, S. Almadani, G. D. Jay, and K. A. Elsaid, "Role of CD44 in Regulating TLR2 Activation of Human Macrophages and Downstream Expression of Proinflammatory Cytokines," *Journal of Immunology* 200 (2018): 758–767.

23. Y. Dong, G. F. T. Poon, A. A. Arif, S. S. M. Lee-Sayer, M. Dosanjh, and P. Johnson, "The Survival of Fetal and Bone Marrow Monocyte-Derived Alveolar Macrophages Is Promoted by CD44 and Its Interaction With Hyaluronan," *Mucosal Immunology* 11 (2018): 601–614.

24. F. Norheim, S. T. Hui, E. Kulahcioglu, et al., "Genetic and Hormonal Control of Hepatic Steatosis in Female and Male Mice," *Journal of Lipid Research* 58 (2017): 178–187.

25. S. Stapleton, G. Welch, L. DiBerardo, and L. R. Freeman, "Sex Differences in a Mouse Model of Diet-Induced Obesity: The Role of the Gut Microbiome," *Biology of Sex Differences* 15 (2024): 5.

26. Y. Yang, D. L. Smith, Jr., K. D. Keating, D. B. Allison, and T. R. Nagy, "Variations in Body Weight, Food Intake and Body Composition After Long-Term High-Fat Diet Feeding in C57BL/6J Mice," *Obesity (Silver Spring)* 22 (2014): 2147–2155.

27. E. Narni-Mancinelli, J. Chaix, A. Fenis, et al., "Fate Mapping Analysis of Lymphoid Cells Expressing the NKp46 Cell Surface Receptor," *Proceedings of the National Academy of Sciences of the United States of America* 108 (2011): 18324–18329.

28. M. Shatirishvili, A. S. Burk, C. M. Franz, et al., "Epidermal-Specific Deletion of CD44 Reveals a Function in Keratinocytes in Response to Mechanical Stress," *Cell Death & Disease* 7 (2016): e2461.

29. C. Luci, E. Vieira, M. Bourinet, et al., "SYK-3BP2 Pathway Activity in Parenchymal and Myeloid Cells Is a Key Pathogenic Factor in Metabolic Steatohepatitis," *Cellular and Molecular Gastroenterology and Hepatology* 13 (2022): 173–191.

30. H. Peng, X. Jiang, Y. Chen, et al., "Liver-Resident NK Cells Confer Adaptive Immunity in Skin-Contact Inflammation," *Journal of Clinical Investigation* 123 (2013): 1444–1456.

31. D. K. Sojka, B. Plougastel-Douglas, L. Yang, et al., "Tissue-Resident Natural Killer (NK) Cells Are Cell Lineages Distinct From Thymic and Conventional Splenic NK Cells," *eLife* 3 (2014): e01659.

32. Y. Fan, W. Zhang, H. Wei, R. Sun, Z. Tian, and Y. Chen, "Hepatic NK Cells Attenuate Fibrosis Progression of Non-Alcoholic Steatohepatitis in Dependent of CXCL10-Mediated Recruitment," *Liver International* 40 (2020): 598–608.

33. R. J. Arguello, A. J. Combes, R. Char, et al., "SCENITH: A Flow Cytometry-Based Method to Functionally Profile Energy Metabolism With Single-Cell Resolution," *Cell Metabolism* 32 (2020): 1063–1075.

34. A. Remmerie, L. Martens, T. Thone, et al., "Osteopontin Expression Identifies a Subset of Recruited Macrophages Distinct From Kupffer Cells in the Fatty Liver," *Immunity* 53 (2020): 641–657.

35. M. Marotel, U. Hasan, S. Viel, A. Marcais, and T. Walzer, "Back to the Drawing Board: Understanding the Complexity of Hepatic Innate Lymphoid Cells," *European Journal of Immunology* 46 (2016): 2095–2098.

36. M. Guilliams, J. Bonnardel, B. Haest, et al., "Spatial Proteogenomics Reveals Distinct and Evolutionarily Conserved Hepatic Macrophage Niches," *Cell* 185 (2022): 379–396.

37. C. Luci, E. Vieira, T. Perchet, P. Gual, and R. Golub, "Natural Killer Cells and Type 1 Innate Lymphoid Cells Are New Actors in Non-Alcoholic Fatty Liver Disease," *Frontiers in Immunology* 10 (2019): 1192.

38. A. C. Tosello-Trampont, S. G. Landes, V. Nguyen, T. I. Novobrantseva, and Y. S. Hahn, "Kuppfer Cells Trigger Nonalcoholic Steatohepatitis Development in Diet-Induced Mouse Model Through Tumor Necrosis Factor-Alpha Production," *Journal of Biological Chemistry* 287 (2012): 40161–40172.

39. S. Tran, I. Baba, L. Poupel, et al., "Impaired Kupffer Cell Self-Renewal Alters the Liver Response to Lipid Overload During Non-Alcoholic Steatohepatitis," *Immunity* 53 (2020): 627–640.

40. A. Remmerie, L. Martens, and C. L. Scott, "Macrophage Subsets in Obesity, Aligning the Liver and Adipose Tissue," *Frontiers in Endocrinology* 11 (2020): 259.

41. K. R. Karlmark, R. Weiskirchen, H. W. Zimmermann, et al., "Hepatic Recruitment of the Inflammatory Gr1+ Monocyte Subset Upon Liver Injury Promotes Hepatic Fibrosis," *Hepatology* 50 (2009): 261–274.

42. C. L. Scott, F. Zheng, P. De Baetselier, et al., "Bone Marrow-Derived Monocytes Give Rise to Self-Renewing and Fully Differentiated Kupffer Cells," *Nature Communications* 7 (2016): 10321.

43. L. Devisscher, C. L. Scott, S. Lefere, et al., "Non-Alcoholic Steatohepatitis Induces Transient Changes Within the Liver Macrophage Pool," *Cellular Immunology* 322 (2017): 74–83.

44. P. J. Murray and T. A. Wynn, "Protective and Pathogenic Functions of Macrophage Subsets," *Nature Reviews. Immunology* 11 (2011): 723–737.

45. J. Chen and L. B. Ivashkiv, "IFN-Gamma Abrogates Endotoxin Tolerance by Facilitating Toll-Like Receptor-Induced Chromatin Remodeling," *Proceedings of the National Academy of Sciences of the United States of America* 107 (2010): 19438–19443.

46. C. Wu, Y. Xue, P. Wang, et al., "IFN-Gamma Primes Macrophage Activation by Increasing Phosphatase and Tensin Homolog via Downregulation of miR-3473b," *Journal of Immunology (Baltimore, Md: 1950)* 193 (2014): 3036–3044.

47. K. U. Saikh, J. S. Lee, T. L. Kissner, B. Dyas, and R. G. Ulrich, "Toll-Like Receptor and Cytokine Expression Patterns of CD56+ T Cells Are Similar to Natural Killer Cells in Response to Infection With Venezuelan Equine Encephalitis Virus Replicons," *Journal of Infectious Diseases* 188 (2003): 1562–1570.

48. N. M. Lauzon, F. Mian, R. MacKenzie, and A. A. Ashkar, "The Direct Effects of Toll-Like Receptor Ligands on Human NK Cell Cytokine Production and Cytotoxicity," *Cellular Immunology* 241 (2006): 102–112.

49. M. F. Mian, N. M. Lauzon, D. W. Andrews, B. D. Lichty, and A. A. Ashkar, "FimH Can Directly Activate Human and Murine Natural Killer Cells via TLR4," *Molecular Therapy* 18 (2010): 1379–1388.

50. L. M. Kanevskiy, W. G. Telford, A. M. Sapozhnikov, and E. I. Kovalenko, "Lipopolysaccharide Induces IFN-Gamma Production in Human NK Cells," *Frontiers in Immunology* 4 (2013): 11.

51. L. M. Kanevskiy, S. A. Erokhina, M. A. Streltsova, et al., "The Role of O-Antigen in LPS-Induced Activation of Human NK Cells," *Journal of Immunology Research* 1 (2019): 2019:3062754.

52. S. A. Freeman, A. Vega, M. Riedl, et al., "Transmembrane Pickets Connect Cyto- and Pericellular Skeletons Forming Barriers to Receptor Engagement," *Cell* 172 (2018): 305–317.

53. S. Papaioannou, J. X. See, M. Jeong, et al., "Liver Sinusoidal Endothelial Cells Orchestrate NK Cell Recruitment and Activation in Acute Inflammatory Liver Injury," *Cell Reports* 42 (2023): 112836.

54. F. Wang, X. Zhang, W. Liu, et al., "Activated Natural Killer Cell Promotes Nonalcoholic Steatohepatitis Through Mediating JAK/STAT Pathway," *Cellular and Molecular Gastroenterology and Hepatology* 13 (2022): 257–274.

55. F. Fasbender, A. Widera, J. G. Hengstler, and C. Watzl, "Natural Killer Cells and Liver Fibrosis," *Frontiers in Immunology* 7 (2016): 19.

56. T. Li, Y. Yang, H. Song, et al., "Activated NK Cells Kill Hepatic Stellate Cells via p38/PI3K Signaling in a TRAIL-Involved Degranulation Manner," *Journal of Leukocyte Biology* 105 (2019): 695–704.

57. C. Gur, S. Doron, S. Kfir-Erenfeld, et al., "NKp46-Mediated Killing of Human and Mouse Hepatic Stellate Cells Attenuates Liver Fibrosis," *Gut* 61 (2012): 885–893.

58. N. Muhanna, L. Abu Tair, S. Doron, et al., "Amelioration of Hepatic Fibrosis by NK Cell Activation," *Gut* 60 (2011): 90–98.

59. C. Luci, S. Bekri, F. Bihl, et al., "NKp46+ Innate Lymphoid Cells Dampen Vaginal CD8 T Cell Responses Following Local Immunization With a Cholera Toxin-Based Vaccine," *PLoS One* 10 (2015): e0143224.

Supporting Information

Additional supporting information can be found online in the Supporting Information section. **Figure S1:** Phenotype and function of liver NK cells and ILC1s. Representative histogram plot showing marker expression on liver ILC1s (red line) and NK cells (blue line) with isotype control (dotted black line). Cell surface expression of KLRG1, CD69, NKG2A, NKG2D were evaluated by flow cytometry after gating on hepatic $CD45^+$ $CD3^-$ $NKp46^+$ $CD49b^+$ NK cells and $CD45^+$ $CD3^-$ $NKp46^+$ $CD49a^+$ ILC1. FMO: fluorescence minus one + isotype control antibody. IFN-γ expression in NK cells and ILC1 was assessed after a 4 h in vitro stimulation assay of hepatic cells with IL-12 + IL-18 by flow cytometry as previously described [6, 59]. Representative histogram plots are shown and bar graph represents mean ± SEM of 1 experiment (3 mice/group). **Figure S2:** Liver NK cells and ILC1 in diet-induced steatohepatitis. (A) Representative dot plots of CD49a and CD49b expression gated on CD45+ CD3− NKp46+ in mice fed with WD or MCDD. (B) NKp46+ ILC, NK cell and ILC1 number evaluated by flow cytometry in livers of NKp46+/+CD44flox/flox and NKp46iCre/+CD44flox/flox mice fed for 24 weeks with chow diet (CD) or Western diet (WD). Histograms represent mean values ± SEM of pooled data from 2 to 3 independent experiments (4–10 mice/group). *p* values are indicated for two-way ANOVA analysis with Benjamini correction. Statistical significance was defined as $p < 0.05$. **Figure S3:** The CXCR3/CXCL10 axis is not involved in CD44 mediated effect on NKp46+ ILCs. Evaluation of CXCR3 expression in hepatic NK cells by flow cytometry and CXCL10 production by ELISA assay in the total liver after 4 weeks of MCDD. Histograms represent mean ± SEM of pooled data from 1 to 3 independent experiments (3–12 mice/group). *p* values are indicated for two-way ANOVA analysis with Benjamini correction. Statistical significance was defined as $p < 0.05$. **Figure S4:** The hepatic macrophage pool and specifically the osteopontin+ subset is regulated by CD44-deficient NKp46+ ILCs during MASH pathogenesis. Number of hepatic OPN+ monocyte-derived macrophages after 24 weeks of Western Diet. Histograms represent mean values ± SEM of pooled data from 2 independent experiments (7–9 mice/group). *p* value is indicated for Mann–Whitney test. Statistical significance was defined as $p < 0.05$. **Figure S5:** CD44 does not regulate the activation of NK cells after stimulation with IL12/IL18. Tlr4 and b2m gene expression in naive liver NK cells evaluated by qPCR (left panel) and expression pattern of Tlr4 in human liver after single-cell RNA sequencing analysis from www.livercellatlas.org (right panel) [36]. (B) NK cell purification/expansion strategy and dot-plots of NK cell isolation according to the different stages of experimentation (NK cell frequency is represented in Q3 framed in red). (C) IFNγ, TNFα, GM-CSF protein levels measured by ELISA assay in the supernatant of NK cells stimulated with IL12 (20 ng/mL) + IL18 (5 ng/mL) during 4 h. Histograms represent mean values ± SEM of pooled data from 1 experiment (3 mice/group). *p* values are indicated for two-way ANOVA analysis with Benjamini correction. Statistical significance was defined as $p < 0.05$. **Figure S6:** Hepatic Eomesodermin expression correlates with Cd44 expression in livers of patients with obesity. Expression pattern of CD44 and Eomesodermin in human liver after single-cell RNA sequencing analysis from www.livercellatlas.org [36]. (B) Liver Cd44 and Eomesodermin mRNA expression levels evaluated by qPCR in patients with morbid obesity without MASLD ($n = 7$) and with MASLD ($n = 13$). Data are presented as mRNA level normalised to the RPLP0 mRNA level. Histograms represent mean value ± SEM. (C) Correlation between hepatic Eomesodermin and hepatic Cd44 expression levels in patients with obesity without (white circles) and with (black circles) MASLD. Linear regression curve, Spearman *r* value, and *p* value (95% confidence interval) are shown. *p* values are indicated for Mann–Whitney test. Statistical significance was defined as $p < 0.05$.